Station Keeping and Rendezvous of an On-orbit Satellite Refuelling System

Joost Ian Hubbard
ID: 210372773
Supervisor: Dr. Angadh Nanjangud

April 24, 2024

Abstract

The increasing commercialisation and expansion of the Low Earth Orbit (LEO) ecosystem are hindered by the limited lifetimes of satellites, primarily due to fuel depletion. The concept of on-orbit servicing, specifically the '*Beyond Fuel*' proposal, addresses this challenge by offering refuelling services to extend the operational lifetimes of satellites. This paper presents the design and simulation of orbit maintenance and rendezvous manoeuvres for a depot satellite and service vehicle. Orbital parameters for the depot were found through Low Earth Orbit population analysis. Utilising both Python and FreeFlyer simulation, orbital decay, station keeping, and rendezvous manoeuvres were modelled. The associated fuel costs for these manoeuvres were also calculated. Consequently, the depot satellite is anticipated to operate in a low eccentricity, Low Earth Orbit at an altitude of 550km and inclined at 53 degrees, requiring 104.2382 kilograms of fuel for 20-year orbit maintenance. The service vehicle requires 182.2057 kilograms for the exemplary rendezvous mission - encompassing inclination and altitude adjustment as well as phasing.

Contents

List of Symbols

Symbol	Description
F_d	Drag force exerted on the satellite by the atmosphere
ρ	Density of the atmosphere at the altitude of the satellite
v	Velocity of the satellite relative to the atmosphere
A	Effective cross-sectional area of the satellite perpendicular to the velocity vector
C_d	Drag coefficient
$\dot{h}$	Change in the satellite's altitude
h	Satellite's altitude
G	Universal gravitational constant
M	Earth's mass
C_D	Drag coefficient of the satellite
A	Surface area of the satellite
m	Mass of the satellite
R_E	Radius of Earth (6371 km)
ρ	Local atmospheric density
v	Velocity
μ	Standard Gravitational Parameter of Earth (398600 km^3/s^2)
r	Radius of the orbit from Earth
a	Orbit semi-major axis
Δv	Change in velocity
I_{sp}	Specific impulse
g_0	Standard gravity
m_0	Wet mass of the satellite
m_f	Dry mass of the satellite
v_1	Initial orbit velocity
v_2	Target orbit velocity
Δi	Angle between planes
θ	Phasing angle

List of Acronyms

GEO Geosynchronous Equatorial Orbit. 2, 14

HST Hohmann Spiral Transfer. 14–17

LEO Low Earth Orbit. , 1–3, 7, 17, 18

MEO Medium Earth Orbit. 2

MSIS Mass Spectrometer Incoherent Scatter. 4–7

ODE Ordinary Differential Equation. 4

RCS Reaction Control System. 15

SRP Solar Radiation Pressure. 3, 7

1 Introduction

When approaching the ecosystem of Low Earth Orbit (LEO), it becomes clear that rapid expansion and commercialisation is hindered by the longevity of satellite lifetimes. Historically, lifetimes are limited by a lack of lifetime extension options when in orbit. In other words, when a satellite is placed into orbit, all the fuel it will ever have is on board. Through analysis of existing databases [31], it can be determined that 82% of satellites in orbit today have an expected lifetime of less than four years.

One of the leading reasons for limited satellite lifetimes is fuel depletion. Once initial fuel is exhausted, orbit maintenance cannot be continued, and the satellite must be decommissioned to not add to the orbital debris fields in LEO. In cases of satellite collisions, with orbital debris or between satellites, the satellite is not voluntarily decommissioned and instead becomes disabled, ultimately reentering due to orbital decay. In both cases, the satellite must be replaced through costly manufacturing and launches. These costs can be estimated to be around $400,000 per satellite, assuming a cost of $1500 per kg using a fully loaded Falcon Heavy [28] with an average launch mass Starlink satellite (260kg) [31].

1.1 Beyond Fuel Proposal

A solution to the complications of satellite replacement is proposed by '*Beyond Fuel*'- an on-orbit refuelling system, positioned in LEO to facilitate lifetime extension services to commercial and governmental satellites. This would act as a service contracted out by satellite operators, removing the need for individual refuelling missions or replacements. Instead, fuel could be launched and stored in orbit until it is delivered to any number of client satellites. Through this, operators can complete lifetime extensions at a reduced cost.

The proposed design would act as a system of two satellites to store and deliver fuel to client satellites. One satellite would act as the depot, maintaining an orbit above the majority of LEO satellites and the major drag region. This would allow for the long-term storage of large quantities of fuel. The second satellite would be a service vehicle, used to transport fuel to clients and remove debris. This would mean separating from the depot to rendezvous with clients or debris and then returning to the depot.

1.2 Aims and Deliverables

Due to the project's complexity, deliverables were created associated with each major component of the proposal. The five components include:

1. A micro-gravity refuelling system focusing on gas-assisted blowdown pumps.
2. A robot arm with associated end effectors.
3. Structural analysis and material choices.
4. A debris de-orbiting system.
5. Design of rendezvous and orbit maintenance manoeuvres for both the depot and service satellite.

This report will focus on the design of the satellite's orbit and the mission plan for on-orbit satellite refuelling. As such, simulations will be bench-marked against industry software such as FreeFlyer and recorded data. A set of deliverables was established to facilitate a logical approach towards these aims.

1. Establishment of orbital parameters for the depot satellite – including altitude, inclination as well as orbit type and class.
2. Analysis and simulation of orbital decay to facilitate the design of maintenance manoeuvres associated with the depot satellite.
3. Design and simulation of rendezvous manoeuvres for use by the service vehicle between the depot and client satellites.
4. Comparison and assessment of varying propulsion systems based upon the chosen manoeuvres.

Alongside this, the project was planned using a Gantt chart that can be found in the appendix section of this report 7.1.

2 Depot

The first component of the refuelling system that must be analysed is the depot satellite. As previously mentioned, there are stringent requirements for the depot and its orbit. Specifically, the orbit must be low enough to be within serviceable range of client satellites while simultaneously minimising the orbital decay. To facilitate this, parameters for the operational orbit and the station-keeping manoeuvres to maintain that orbit must be designed.

2.1 Orbital Parameters

The initial design parameters for the depot satellite concern its operational orbit, specifically the Keplerian elements. Accurate and careful design of this orbit is instrumental in ensuring the system can operate as proposed.

Proximity to clientele is a primary concern - minimising the required fuel to deliver refilling services on a frequent basis. As a result, analysis of potential client satellites can be used to provide a range of potential parameters for application on the depot. Specifically, the modal orbit class (the altitude range), orbit type (the specific configuration or trajectory pattern) and orbit parameters (the eccentricity, inclination, perigee and apogee) must be investigated.

Making use of recent satellite databases, such as the Union of Concerned Scientists' satellite database [31], orbital data can be analysed for the operational population of the earth's orbit. Relevant tabulated information gained through analysis is displayed below in tables 2, 3 and 4.

Table 2: Satellite population by orbit class.

Orbit Class	Population
LEO	5937
GEO	580
MEO	142
Elliptical	59

Table 3: LEO satellite population by orbit type.

Orbit Type	Population
Non-polar inclined	3641
Sun-synchronous	1506
Polar	748
Elliptical	8
Other	34

Table 4: LEO mode orbital parameters.

Parameter	Value
Perigee (km)	548
Apogee (km)	541
Eccentricity	9.39E-4
Inclination (degrees)	53

When appropriately displayed, it is clear that the most common orbit class is a low earth orbit. This is to be expected since the vast majority of satellites in orbit are used for communications and as such require minimal latency. Assuming LEO to be the most common orbit type, further data analysis reveals that the most common orbit type is a non-polar inclined orbit. In terms of the modal orbital parameters, the average altitude is deemed 545km with approximately zero eccentricity (perfectly circular orbit) and a 53-degree inclination.

Based on this data, the orbital parameters of the depot can be established. Since the service vehicle is required to rendezvous with these satellites, its initial launch point, the depot satellite, must be in a similar orbit – minimising the distance over which the payload will have to travel. Because of this, it can be assumed that our depot satellite will have a circular, LEO with an altitude of 550km and inclined at 53 degrees.

2.2 Simulation Theory: Orbital Decay

A significant obstacle in the development of long-term fuel storage is the orbital decay of the depot over time. After a satellite is placed into its permanent orbit, without active maintenance, it will begin to decay - ultimately reentering the Earth's atmosphere. This occurs due to the various forces which act on a satellite while it orbits the planet - namely drag and gravity.

The drag experienced by satellites in LEO can be separated into two main origins - atmospheric drag and solar radiation pressure. Atmospheric drag, commonly referred to as aerodynamic drag, is experienced by any moving object within an atmosphere; the satellites in LEO are positioned in the upper portions of Earth's atmosphere such as the thermo or exo-sphere. As a result of this, while being minimal compared to very low altitudes, aerodynamic drag is the major drag component acting on the satellite. Solar radiation pressure (SRP) is a component of LEO drag which varies with solar activity.

2.2.1 Atmospheric Drag

As a satellite orbits around the Earth, it collides with any air molecules in its path - each molecule exerting a force opposing the motion of the satellite. In LEO the density of the atmosphere is high enough to impart a significant resistance to motion in this manner. At times of high solar activity, the density of the atmosphere at a specific point increases. This occurs since additional energy is absorbed into the atmosphere and as such low-density layers rise and are replaced by more dense layers - the result of gas thermal expansion. In this case, an LEO satellite would have to travel through a denser atmosphere at the same altitude - increasing the aerodynamic resistance exerted on it [23]. The estimation of atmospheric drag relies on both the structural features of the satellite and the atmospheric density surrounding the satellite in question. The density of the atmosphere at a specific altitude above the earth must be determined based on solar activity and standard atmospheric density models. The structural characteristics, namely the effective surface area, can be described through a wing-box macro model - separating the satellite into the main body and the satellite array [19]. Using these two parameters, the atmospheric drag acting on the satellite can be determined at a point in time and then propagated across a chosen timescale.

The equation used to determine the atmospheric drag force on the satellite is shown below:

$$F_d = \frac{1}{2}\rho v^2 A C_d \tag{1}$$

2.2.2 Solar Radiation Pressure

Solar Radiation Pressure (SRP) describes the absorption and reflection of solar radiation at the satellite's surface [34] - through collisions with photons in the satellite's orbital path. As a result of these interactions, kinetic energy is lost from the satellite - decelerating its motion. While SRP represents one of the most relevant perturbation sources when in deep space [6], in LEO this force is orders of magnitude smaller than aerodynamic drag. As a result of this, SRP can be ignored for proprietary simulation for the sake of simplicity.

2.2.3 Decay Feedback

Regardless of the origin, any drag force exerted on the satellite will cause it to decelerate over time. As a result of this, the altitude of the satellite will reduce until such a time that the altitude is so low that it re-enters the atmosphere - at which point atmospheric drag is so great that the satellite is no longer orbiting. The process of orbital decay, described in the block diagram below 1, is an exponential one. As the satellite drops to a lower altitude, the atmospheric density increases exponentially, leading to increased drag and deceleration until the satellite burns up [25].

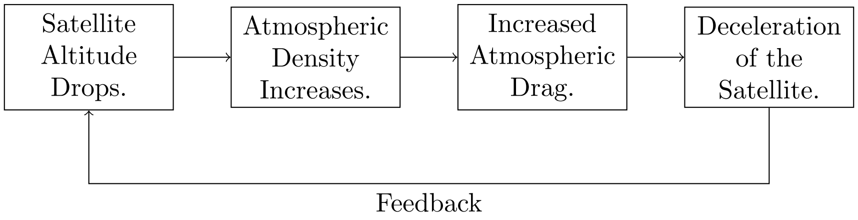
Satellite Altitude Drops.
Atmospheric Density Increases.
Increased Atmospheric Drag.
Deceleration of the Satellite.
Feedback

Figure 1: Orbital decay feedback loop associated with Low Earth Orbit satellites

To numerically simulate this process an ordinary differential equation was derived for the altitude of the satellite above the Earth's surface. Equation 22, derived in appendix section 7.2, can be found below:

$$\dot{h} = -\frac{GMC_D A}{m}\sqrt{R_E + h\rho} \tag{21}$$

2.3 Satellite Lifetime Simulation

Based on the previously derived Ordinary Differential Equation (ODE), a simulation for orbital decay was created. This simulation modelled the altitude of a chosen satellite over a specified time and number of time steps. When modelling the orbital decay, certain assumptions were made to simplify the problem. As discussed in the theory section, a circular orbit was assumed, with drag being taken as just atmospheric.

Since the simulation focused on atmospheric drag, the density of the atmosphere was a key parameter. To ensure the accuracy of atmospheric density the Mass Spectrometer Incoherent Scatter (MSIS)-90 model was chosen - with values being generated from the UK Solar System Data Centre [21]. This model, developed initially in 1987 by A E Hedin [14] and then extended in 1991 [13], makes use of recorded mass spectrometer data from various satellites and on incoherent scatter radar data from several sites on Earth. This allows for relative accuracy up to 700km altitude on a specific date.

Using this model, a Python script was created to simulate orbital decay 7.3. The simulation is a function of the satellite's initial height, mass, drag coefficient and effective surface area. Making use of '*solve.ivp*' from the '*SciPy*' library [33], the ordinary differential equation for the satellite's altitude is numerically evaluated using the Runge–Kutta–Fehlberg method. This determines the loss of orbital energy over time and thus the reduced altitude. It is key to note that, due to the rotation of the satellite undergoing orbital decay, the drag coefficient varies across the decay. The simplification of this as a constant drag coefficient assumes the satellite has a constant effective area and is thus taken as a source of error in the simulation. Nonetheless, a block diagram of the code is shown below displaying the logic of the system.

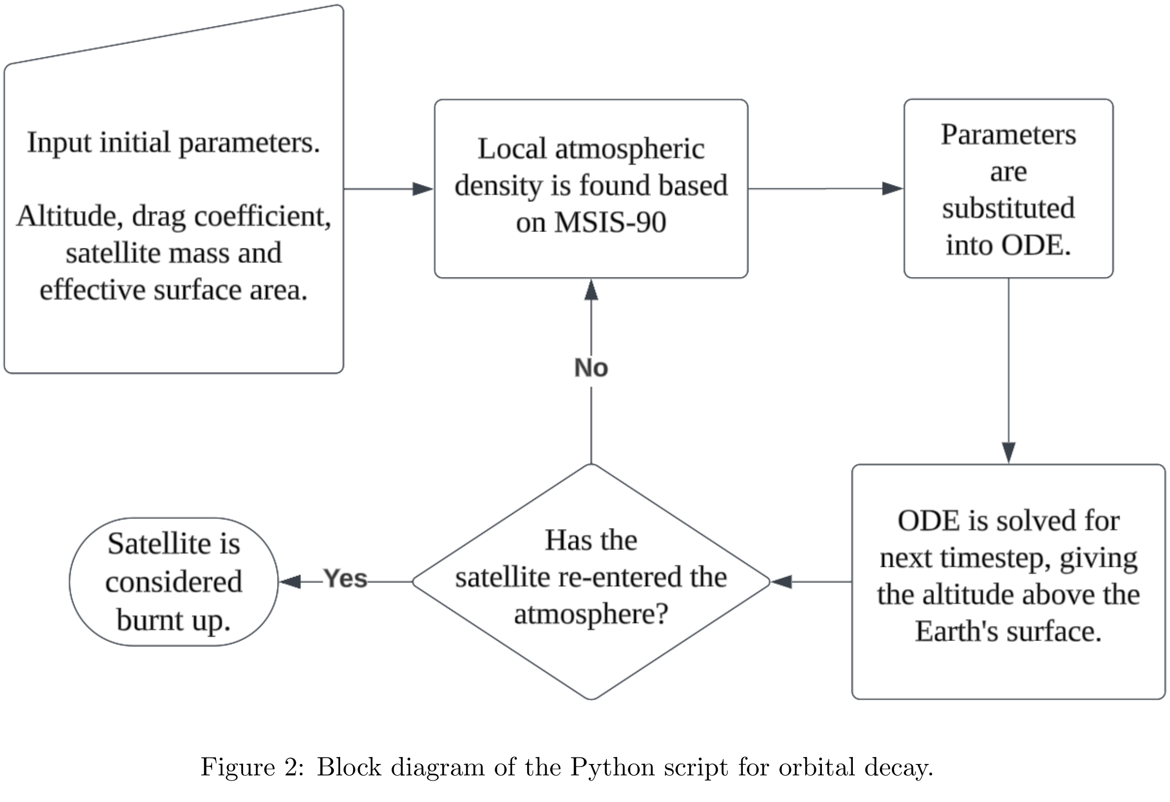
Input initial parameters.
Altitude, drag coefficient, satellite mass and effective surface area.
Local atmospheric density is found based on MSIS-90
Parameters are substituted into ODE.
ODE is solved for next timestep, giving the altitude above the Earth's surface.
Has the satellite re-entered the atmosphere?
No
Yes
Satellite is considered burnt up.

Figure 2: Block diagram of the Python script for orbital decay.

2.3.1 Simulation verification

To verify the accuracy of the Python simulation, it was compared to real satellite data - the orbital decay and subsequent uncontrolled reentry of Tiangong-1. The satellite was launched from Jiuquan Satellite Launch

Center on September 30^{th}, 2011. On March 16^{th}, 2016, China reported Tiangong-1 had “ceased functioning” and as such the satellite had begun to decay. This ultimately led to an uncontrolled reentry on the April 2^{nd} 2018 [8]. An orbital decay plot for the last part of reentry can be seen below in figure 3 for later comparison to the simulation plot - indicating a decay time of 750 days.

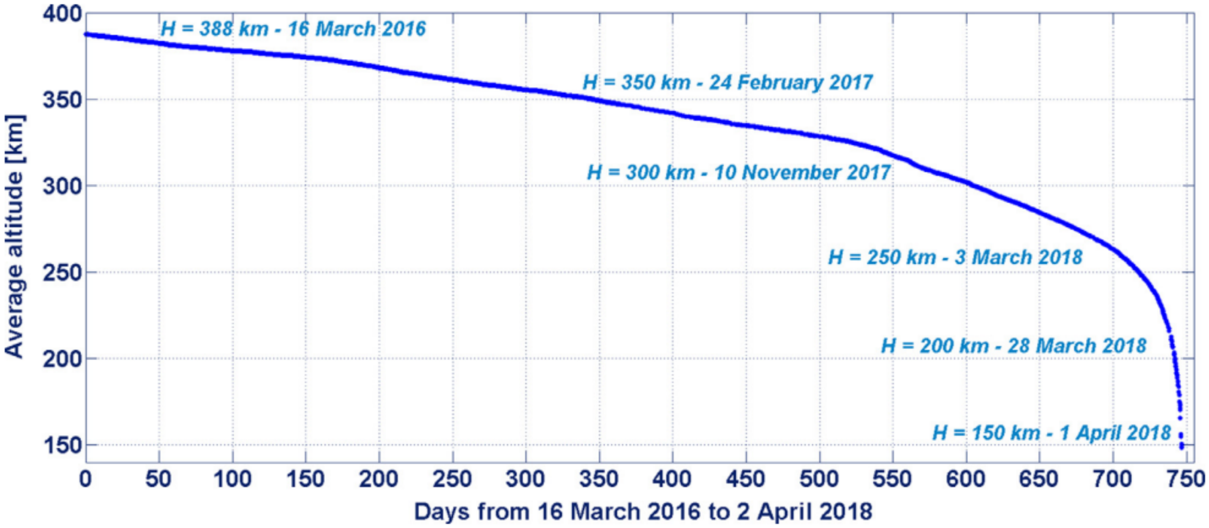

Figure 3: Altitude plot of the Tiangong-1 satellite from satellite data [27].

To ensure the simulation was completed accurately, the correct parameters must be used 5.

Table 5: Tiangong-1 simulation input parameters.

Initial Altitude	**Satellite Mass**	**Drag Coefficient**	**Effective Surface Area**
380 km	7500 kg	2.2	34.84 m^2

Aside from the physical parameters, the density model remains to be defined. The bulk of Tiangong-1’s orbital decay occurred across 2017 - with minor parts being in late 2016 and early 2018. The density model chosen must reflect the atmospheric conditions over this period - taking into account solar activity at the time. To ensure this was done accurately, density data for this case study was taken from the midpoint of the time period (March 24^{th} 2017). This data was retrieved from the MSIS-90 model [21] and is displayed below in figure 4.

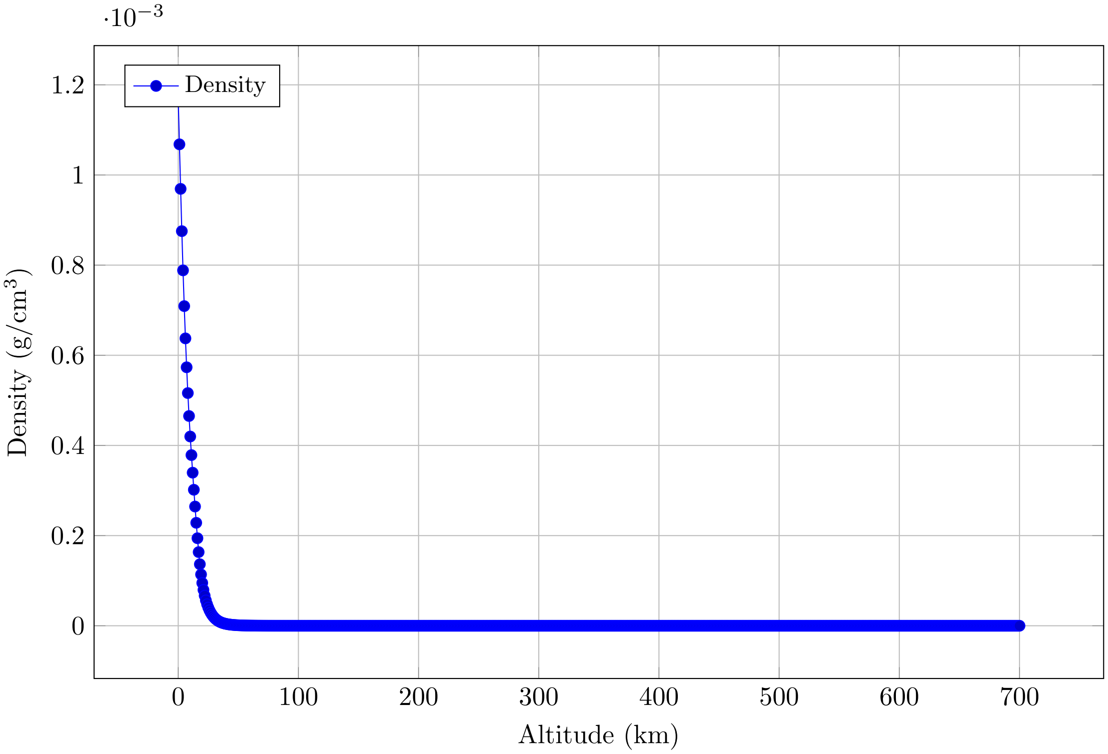

Figure 4: Density variation with altitude on March 24th 2017 from Mass Spectrometer Incoherent Scatter-90 [21].

Making use of these parameters and density model, the orbital decay of Tiangong-1 can be simulated in Python as shown in figure 5.

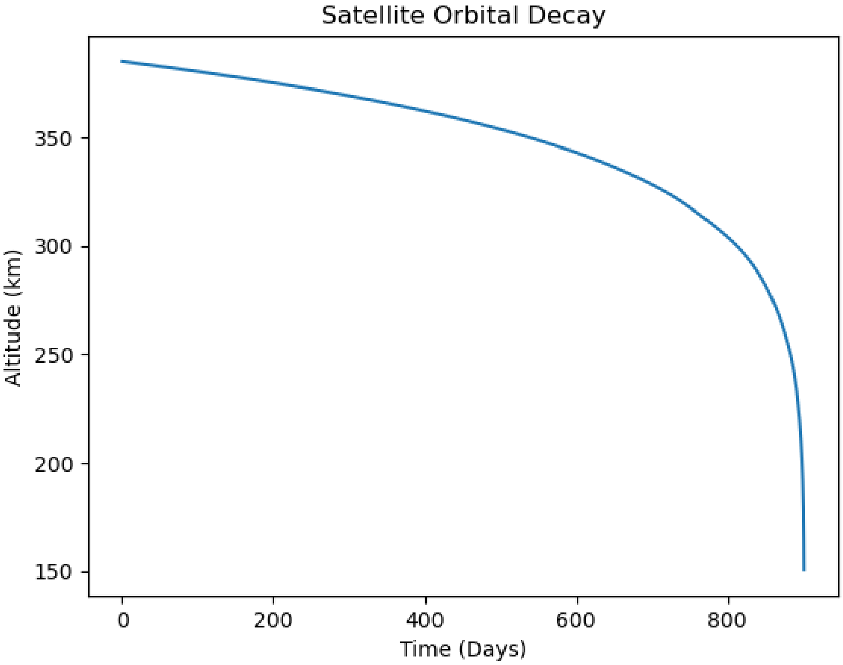

Figure 5: Altitude plot of the Tiangong-1 satellite from Python simulation.

A brief analysis indicates a good level of agreement between the simulation and real orbital decay plots. Both graphs display a similar profile with a rapidly growing rate of decay as the satellite enters denser sections of the atmosphere. The actual time to decay is slightly faster, with an 18.35% difference in the time of reentry (taking 901 days in the Python prediction). This disparity can explained by three simplifications made for the simulation:

1. **Constant effective area.** To assume that effective area is constant, it must also be assumed that the satellite does not rotate during its decay - changing the surface experiencing aerodynamic drag. This is not true and can lead to disparity with real datasets.
2. **Ignorance of Solar Radiation Pressure.** The lack of SRP in the decay simulation reduces the total drag acting on the satellite. While the effect in LEO is minimal, the difference in drag could lead to slower decay over long periods.
3. **Constant density model.** The assumption that the density model is constant across the decay period is inaccurate due to variance in solar conditions. Although variances may be small, they could lead to disparities in results over extended periods, affecting decay times in response to fluctuations in solar activity.

Over a longer period, these differences can become much more pronounced, as illustrated by the projected decay of a CubeSat orbiting at 600km, as discussed in the paper 'How long does it take for a satellite to fall to Earth?' [17]. The paper highlights that commonly used prediction tools in the industry, like NASA's Debris Assessment Software [24], which factor in solar radiation pressure and geomagnetic activity, forecast significantly reduced lifespans - for the CubeSat, from approximately 32 years to 18 years.

In the interest of accuracy, a second decay simulation was run using the FreeFlyer software, once again making use of a MSIS-90 density model and the Runge–Kutta–Fehlberg method for propagation.

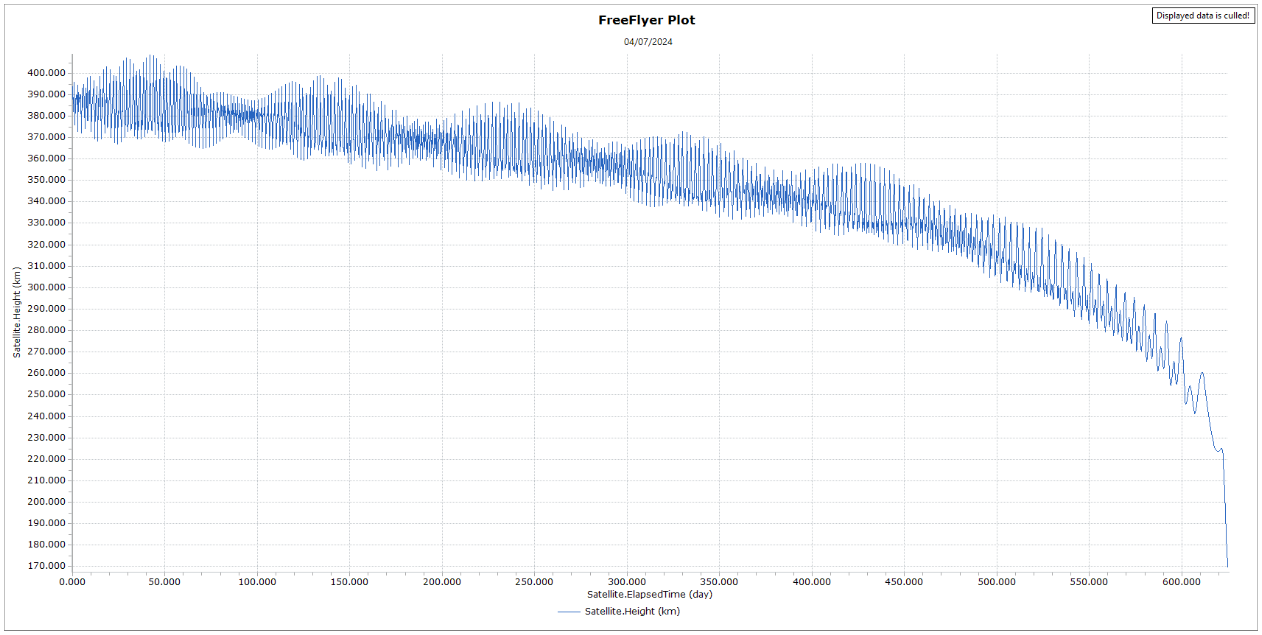

Figure 6: Altitude plot of the Tiangong-1 satellite from FreeFlyer simulation.

This resulted in a decay plot (6) being produced with a time to reentry of 625 days. This means an almost equal error to the Python script of 17.9% when compared to satellite data. This error is an undershoot while the Python simulation was an overshoot.

2.3.2 Depot Lifetime Simulation

Making use of the validation tests completed prior, it is clear that a reasonably accurate lifetime estimation can be made through the comparison of the Python and FreeFlyer simulations. To complete these simulations, the relevant physical parameters are listed below in table 6.

Table 6: Depot satellite simulation input parameters.

Initial Altitude	**Satellite Mass (Including Payload)**	**Drag Coefficient**	**Effective Surface Area**
550 km	15000 kg	2.2	36.55 m^2

Based on these parameters the orbital decay of the depot satellite can be predicted as shown in figures 7 and 8.

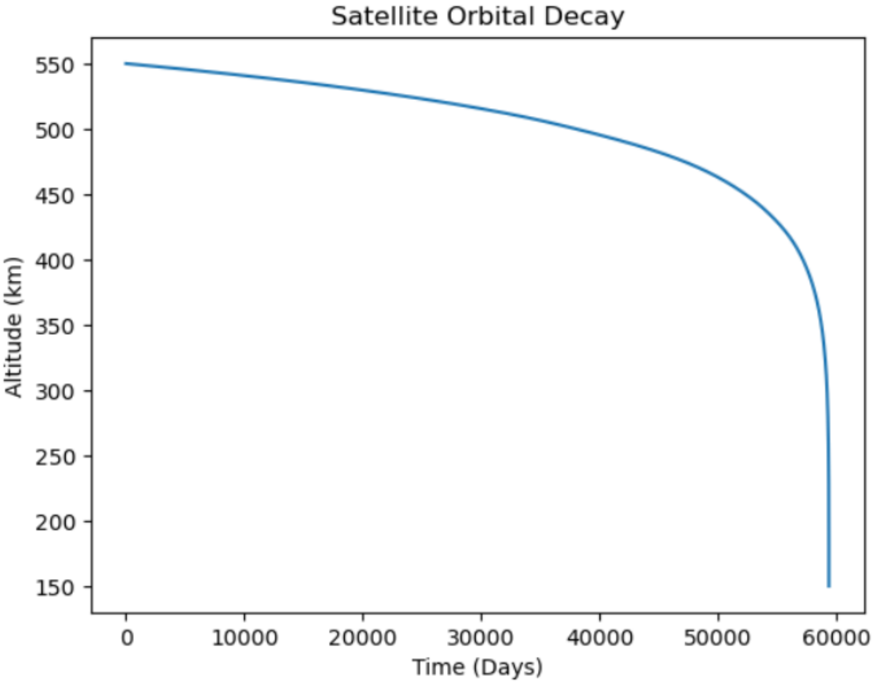

Figure 7: Altitude plot of the depot satellite from Python simulation.

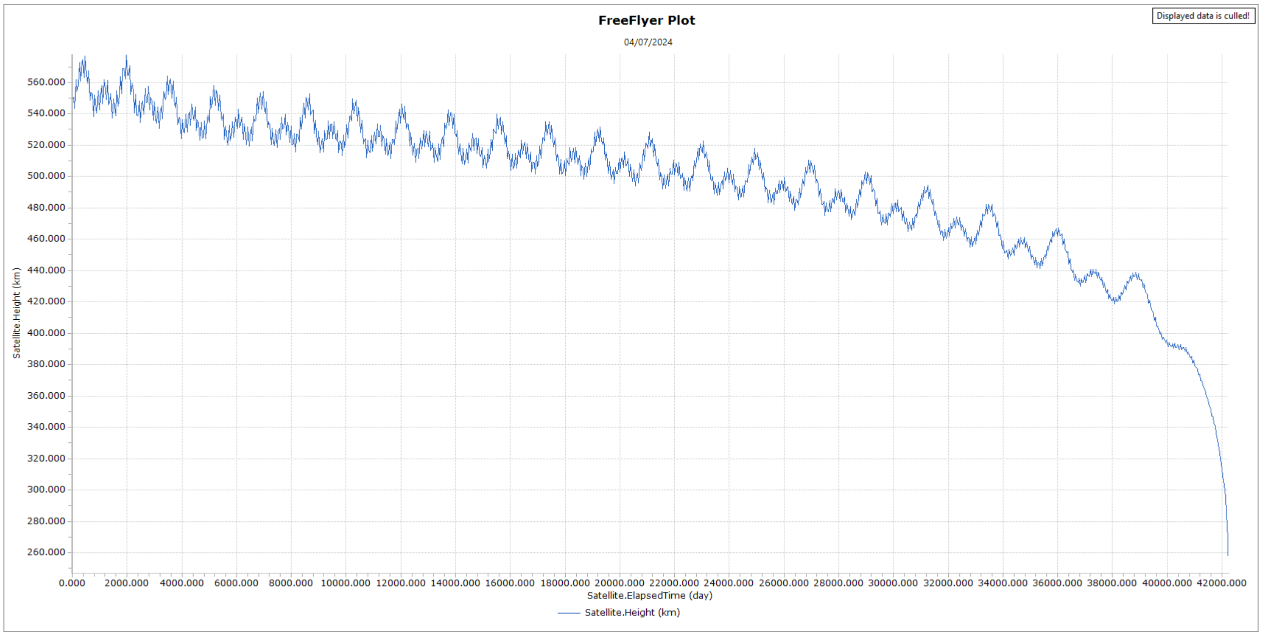

Figure 8: Altitude plot of the depot satellite from FreeFlyer simulation.

Through initial analysis of these plots, it can be seen that the Python simulation predicts a lifetime of 59341 days while the FreeFlyer simulation predicts a lifetime of 42324 days. As before, it can be assumed the true lifetime of the depot can be found at the midpoint between the two values - giving a lifetime of 50832.5 days.

2.4 Station-keeping

To mitigate orbital decay, orbit maintenance, or station-keeping manoeuvres are used. These typically take the form of propellant burns to raise the altitude of the satellite when it falls below a certain altitude threshold or tolerance. Various methods can be used to achieve this, with the deciding factor between them being fuel efficiency. Due to the importance of weight and longevity when designing a satellite, the chosen manoeuvre must complete the required objective with a minimal delta-v cost thus requiring minimal fuel. This ensures minimal space and weight allocation to the satellite's fuel storage while providing longevity to its lifetime.

Once more Tiangong-1 offers a cautionary case study, emphasising the significance of station-keeping throughout the operational lifespan of a satellite. Before control loss, the satellite regularly undertook orbit maintenance manoeuvres to maintain a stable orbit between 350 and 400 km. When these manoeuvres became impossible to continue, the satellite underwent catastrophic decay and reentry as discussed previously. Evidence of these manoeuvres can be seen below in figure 9.

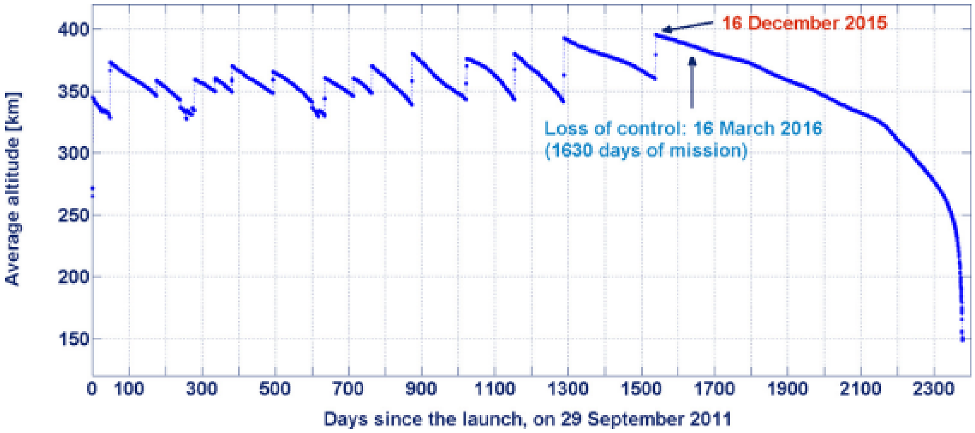

Figure 9: Evolution of the average altitude of Tiangong-1 across its lifetime [27].

2.4.1 Simulation Theory: Types of Transfer

To determine the appropriate orbit maintenance manoeuvre for the depot satellite, two methods and their associated delta v costs were evaluated. The methods compared were a Hohmann and a Bi-elliptic transfer.

The process of a Hohmann transfer involves a series of steps to transition a satellite from a lower orbit to a higher one. Initially, Python code was developed to calculate the required delta-v for this transfer. The transfer comprises three main phases:

1. **Initial prograde burn:** This stage involves accelerating the satellite, elongating its orbit into an elliptical shape with the desired altitude as its apoapsis.
2. **Coasting phase:** Following the initial burn, the spacecraft enters a coasting phase, where it follows the elliptical orbit until it reaches the apoapsis.
3. **Second prograde burn:** Once at the apoapsis, the spacecraft executes another prograde burn. This manoeuvre circularises the orbit at the new, higher altitude.

For the Bi-elliptic transfer, a slightly different approach is used. In this case, three burns are used to increase the altitude, described as follows:

1. **Initial prograde burn:** This stage involves accelerating the satellite, elongating its orbit into an elliptical shape with the desired altitude as its apoapsis.

2. **Coasting phase:** Following the initial burn, the spacecraft enters a coasting phase, where it follows the elliptical orbit until it reaches the apoapsis
3. **Second prograde burn:** Once at the apoaspis, a second prograde burn increases the perigee altitude.
4. **Retrograde burn:** Once at the periapis, the spacecraft executes another retrograde burn. This manoeuvre circularises the orbit at the final, higher altitude.

The validity of both approaches was confirmed and visualised using FreeFlyer software, applying the same underlying logic. In both the Python code and FreeFlyer simulations, calculations were based on the vis-viva equation below:

$$v = \sqrt{\mu\left(\frac{2}{r} - \frac{1}{a}\right)} \tag{2}$$

To calculate the delta v associated with the depot satellite undertaking both a bi-elliptic and Hohmann transfer, the vis-viva equation is utilised. This method allows for the calculation of the delta v required for each burn in sequential order and ultimately the total delta-v [2][1].

2.4.2 Simulation

In both cases, an operational altitude of 550 km was specified with a tolerance of 20km. The satellite was modelled as the depot - with parameters detailed in table 6. The velocities of the initial and final orbits are determined to be 7.585 km/s and 7.59 km/s respectively - using equation 2.

Table 7: Delta v cost per orbit maintenance manoeuvre.

	Hohmann Transfer	**Bi-elliptic Transfer**
Total Delta v (km/s)	0.01097	2.357

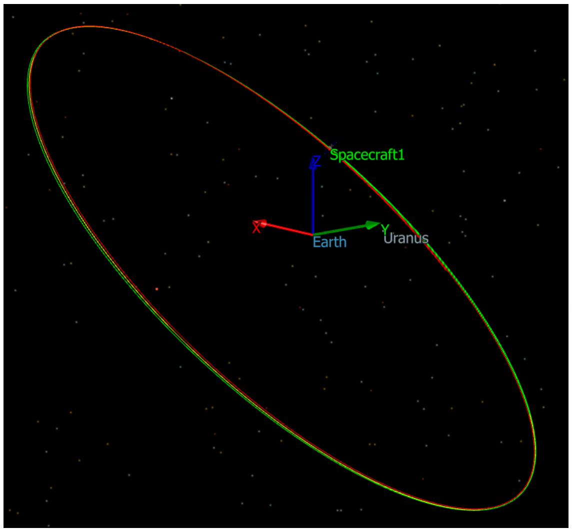

Figure 10: Hohmann transfer visualised in FreeFlyer.

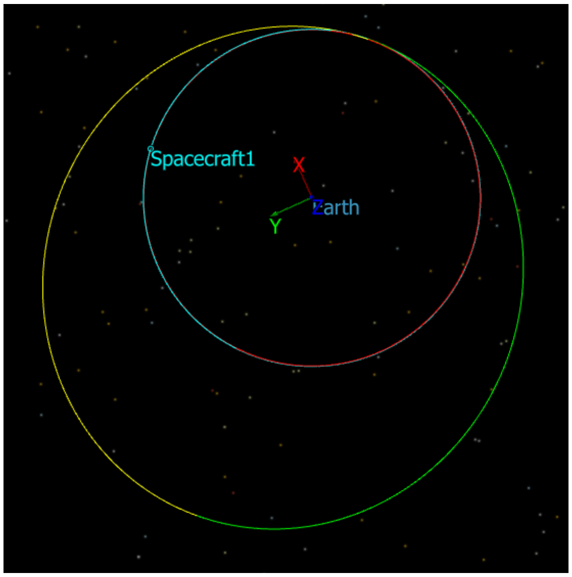

Figure 11: Bi-elliptic transfer visualised in FreeFlyer.

The results of both simulations are tabulated for comparison 7. From this, it can be determined that the Hohmann transfer uses significantly less delta-v than the bi-elliptic transfer for the orbit maintenance of the depot. This is an expected result due to the radii ratio between the chosen and tolerance orbits. When the target orbit to tolerance orbit radii-ratio is less than 15·58 but greater than approximately 11·94, the bi-elliptical transfer is more economical if the intermediate point is placed at a sufficiently high altitude.

[15]. Since the radii ratio in the case of the depot is only slightly above 1 a significant reduction in delta v cost is expected to be found using a Hohmann transfer. This also happens to align with the tests that are conducted in '*Assessment of Orbit Maintenance Strategies for Small Satellites*' [18] in which Hohmann transfers are found be be very efficient.

2.5 Depot Fuel Estimation

The fuel required for the satellite to complete orbit maintenance manoeuvres is a key value that must be defined. To determine this, the total required delta v across a set period must be found alongside the assignment of propulsion systems to the satellite - providing a specific impulse value. Once these values are found, the fuel mass required for the period can be determined using a rearranged ideal rocket equation. The ideal rocket equation [5] is given by:

$$\Delta v = I_{sp} \times g_0 \times \ln\left(\frac{m_0}{m_f}\right) \tag{3}$$

Rearranging the ideal rocket equation for m_0, we get:

$$m_0 = m_f \cdot e^{\frac{\Delta v}{I_{sp} \times g_0}} \tag{4}$$

2.5.1 Delta v

To establish the required delta v for the depot satellite a period of 20 years (7305 days) was chosen. This provides a large enough timescale to be feasible when designing fuel requirements. Using, the previously made Hohmann transfer simulation in FreeFlyer, a new script was created to simulate the orbit maintenance of the satellite to combat orbital decay. This used the same parameters as in the previous depot simulations - found in table 6.

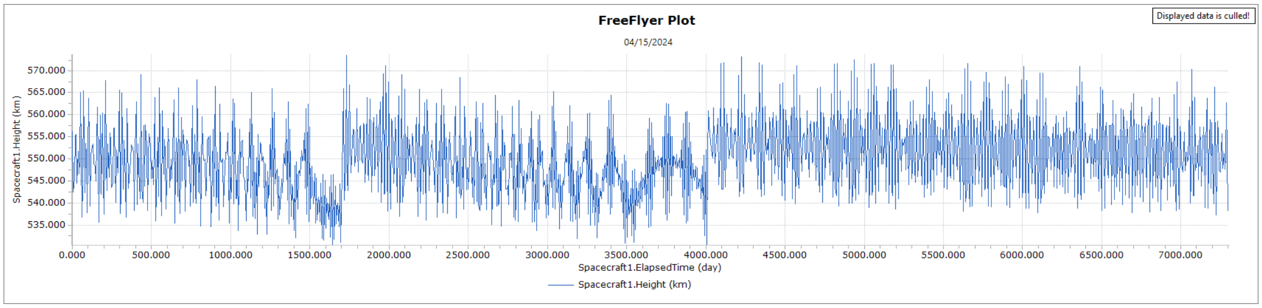

Figure 12: Altitude plot of the depot satellite over 20 years.

From figure 12, it can be seen that 2 Hohmann transfers are required across 20 years to maintain a stable orbit at 550 km altitude. From this, it can be determined that the required delta v for one year is $0.0109\,\text{km/s} \times 2 = 0.0218\,\text{km/s}$.

2.5.2 Propulsion system

The determination of a specific propulsion system within the depot satellite is crucial to determine the fuel requirements. This is because the type of propulsion system defines the specific impulse (I_{sp}) available. To establish the appropriate system, a weighted decision matrix was created based on literature sources - as seen below in figure 8.

Table 8: Depot satellite propulsion system weighted decision matrix [32] [20].

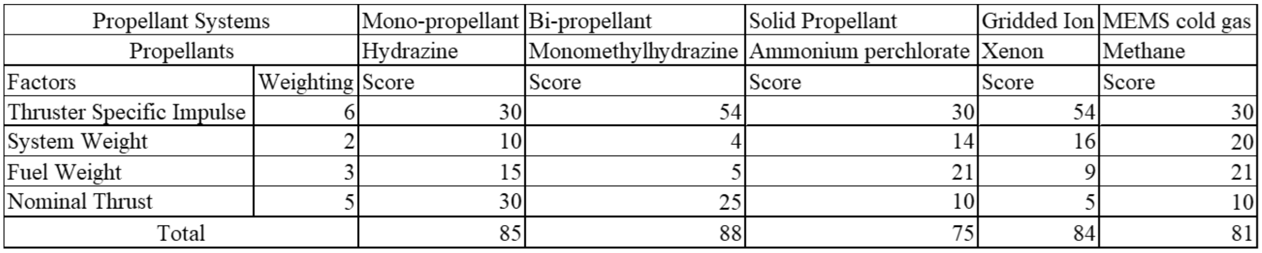

Propellant Systems		Mono-propellant	Bi-propellant	Solid Propellant	Gridded Ion	MEMS cold gas
Propellants		Hydrazine	Monomethylhydrazine	Ammonium perchlorate	Xenon	Methane
Factors	Weighting	Score	Score	Score	Score	Score
Thruster Specific Impulse	6	30	54	30	54	30
System Weight	2	10	4	14	16	20
Fuel Weight	3	15	5	21	9	21
Nominal Thrust	5	30	25	10	5	10
Total		85	88	75	84	81

From this, it is clear that a chemical bi-propellant system is ideal for application on the deport satellite. Typically, these systems provide a high specific impulse while limiting system and fuel weight. The nominal thrust associated with bi-propellant systems is lower than that of solid systems but in this case will suffice. This is because the depot satellite will be under micro-gravity and as such will have a lower gravitational force opposing any station-keeping manoeuvres. It is worth noting that if a higher thrust was required for any reason, the propellant choice could be adjusted to increase its mass. This is because a higher fuel weight is intrusively linked to the thrust produced by a thruster [7].

In terms of a specific propulsion system, the 400N Bi-Propellant Apogee Motor by AirianeGroup was chosen. The key specifications are detailed below **??**.

Table 9: Depot satellite propulsion system specifications [4]

Parameter	**Value**
Nominal Thrust	425 N
Nominal Specific Impulse	321 s
Mass	4.3 kg
Fuel	Monomethylhydrazine
Oxidizer	N2O4, MON-1, MON-3

2.5.3 Fuel Mass

Finally, the fuel mass required for the deport satellite to conduct orbit maintenance over 20 years can be determined. The delta-v cost across the 20-year period is found to be 0.0218 km/s while the specific impulse of the satellite is given as 321 seconds. Making use of equation 2.5 the required total mass of the satellite including required fuel can be determined:

$$m_0 = 15000\,\text{kg} \cdot e^{\frac{0.0218\times10^3\,\text{m/s}}{321\,\text{s}\times9.81}} = 15104.2382\,\text{kg}$$

From this, it is clear that 104.2382 kilograms of fuel is required to perform orbit maintenance of the deport satellite over 20 years.

3 Service Vehicle

To facilitate the delivery of fuel and removal of debris, a secondary service vehicle will be used. This smaller vehicle will contain a fuel pump, onboard fuel storage tanks and a robotic arm - in addition to basic propulsion and power systems. Using these systems, the depot satellite can remain at a higher altitude to store more fuel mass while a lighter and more agile vehicle can provide the services at varied altitudes.

This section of the report will detail the steps taken by the service vehicle to conduct rendezvous manoeuvres with an example satellite - resulting in a calculated fuel cost. This should allow for general fuel sizing for a potential mission.

3.1 Phases of a Rendezvous Mission

The rendezvous process consists of a series of orbital manoeuvres which bring the chaser satellite into the vicinity of the target - eventually allowing for docking between the two vehicles [10]. The standard approach to rendezvous follows a series of phases as detailed below in figure 13.

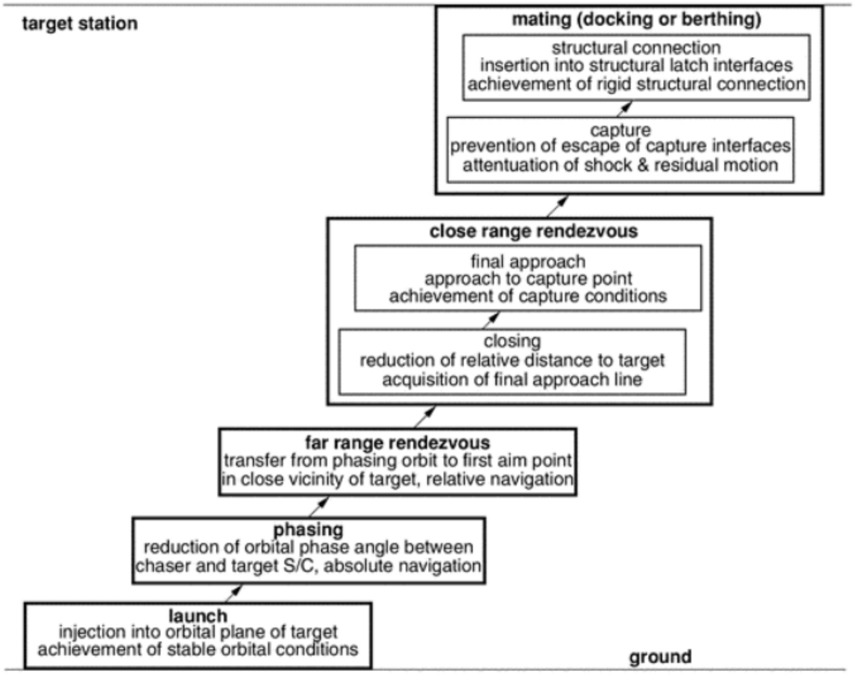
target station
mating (docking or berthing)
structural connection
insertion into structural latch interfaces
achievement of rigid structural connection
capture
prevention of escape of capture interfaces
attentuation of shock & residual motion
close range rendezvous
final approach
approach to capture point
achievement of capture conditions
closing
reduction of relative distance to target
acquisition of final approach line
far range rendezvous
transfer from phasing orbit to first aim point
in close vicinity of target, relative navigation
phasing
reduction of orbital phase angle between
chaser and target S/C, absolute navigation
launch
injection into orbital plane of target
achievement of stable orbital conditions
ground

Figure 13: Main phases of a typical rendezvous mission [10].

3.1.1 Launch

The launch phase can be ignored for the service satellite. This is because, before use, the vehicle is docked within the depot satellite, meaning it is already in the same orbit as the depot.

3.1.2 Far-range Rendezvous

The far-range rendezvous phase is the transition from the phasing orbit to an orbit close to that of the target. If the chaser and target satellites are both positioned in low eccentricity orbits with different altitudes, co-planar rendezvous manoeuvres can be used to manoeuvres the chaser [12]. This is often done using Hohmann transfers to ensure delta-v efficiency.

In addition to altitude adjustment, inclination differences must be accounted for between the chaser and client satellites. Commonly referred to as a 'plane change' manoeuvre, changing the inclination of the chaser satellite can be done through a simple impulsive burn - as shown in 18. In this case, the shape of the initial orbit will not change.

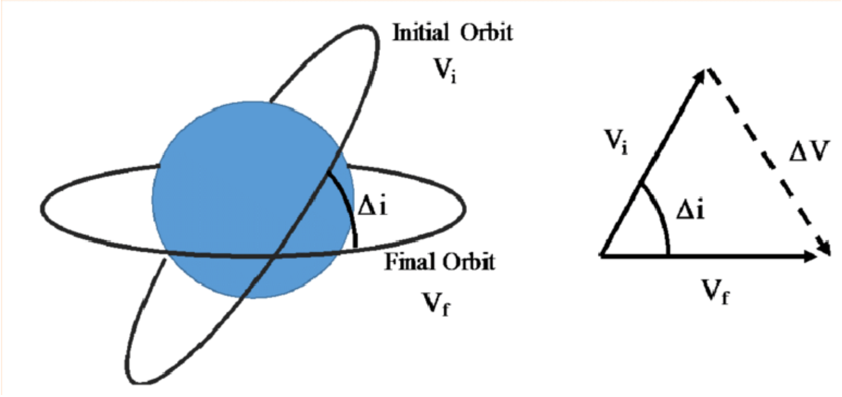

Figure 14: Generic geometry of a plane change manoeuvre [3].

In the case where both an inclination change and an altitude adjustment are required, a Hohmann Spiral Transfer (HST) can be used. This manoeuvre combines both components of the far-range rendezvous into one. To ensure delta-v efficiency, the graph below details the benefit region for using a HST.

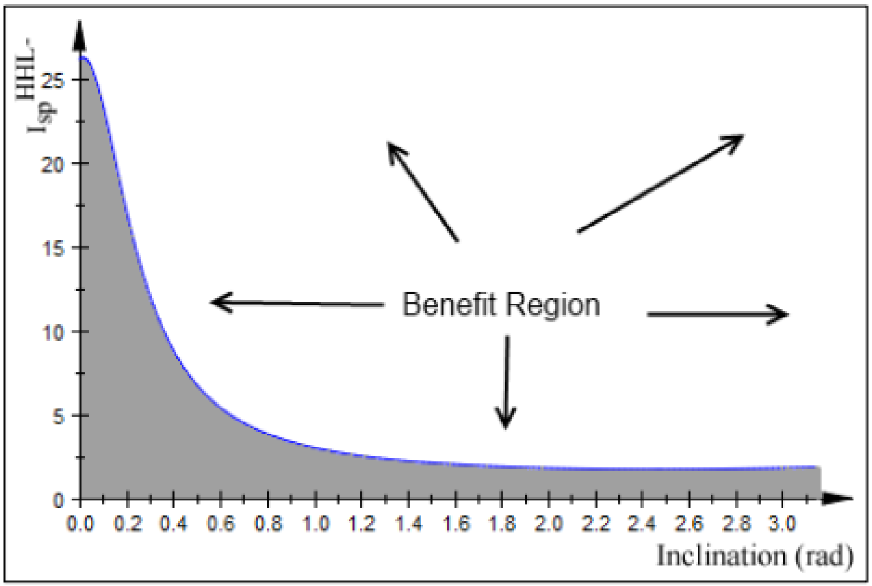

Figure 15: Benefit region for a HST manoeuvres based on inclination change and specific impulse [26].

3.1.3 Phasing

The phasing component of a rendezvous mission plays a significant role in closing the gap between the chaser and target satellites. Phasing manoeuvres are used to change the position of a spacecraft in its orbit and can be used to move two satellites closer together - providing they are in different positions with respect to time along an orbital path. These manoeuvres can also be used by satellites in GEO to relocate to new positions above the Earth [9].

In general, two burn Hohmann transfers are used to conduct the phasing - one burn to enter and leave the transfer orbit respectively. Should a satellite wish to move to a target behind its current position, it can move to a transfer orbit with a higher period than its current orbit and then rejoin its initial orbit at the specified point. If the satellite has a target ahead of it's position, then a transfer orbit with a lover period can be used similarly.

3.1.4 Close-range Rendezvous and Capture

The final approach of the chaser satellite to the target is conducted using the Reaction Control System (RCS) mounted on board. Generally, this means the use of a combination of large and small thrusters for translations and attitude control - in some cases, the attitude is managed purely by reaction wheels or control moment gyroscopes to reduce fuel use.

For the sake of this report, close-range attitude adjustments can be ignored. This is because once the service vehicle is within proximity of the target, the robot arm mounted on the vehicle will perform soft capture.

3.2 Delta-v Calculation

To simulate a potential rendezvous manoeuvre to be conducted by the service vehicle, orbital parameters for the service vehicle and potential target satellite must be defined.

3.2.1 Input Parameters

In this case, making use of the Union of Concerned Scientists' satellite database, a Starlink satellite is chosen - with parameters detailed below in table 10.

Table 10: Starlink-5200 satellite specifications.

Parameter	**Value**
Current Official Name of Satellite	Starlink-5200
Class of Orbit	LEO
Type of Orbit	Polar
Longitude of GEO (degrees)	0
Perigee (km)	358
Apogee (km)	362
Eccentricity	2.97×10^{-4}
Inclination (degrees)	70
Period (minutes)	91.8
Launch Mass (kg)	260
Date of Launch	9/13/2021
Expected Lifetime (years)	4

Starlink-5200 is a communications satellite with a lifetime of around 4 years - making it a prime client for refuelling. This satellite is positioned in LEO with an almost circular orbit. It is in a polar orbit with an inclination of 70 degrees.

In terms of the service satellite, the orbital parameters for its orbit will be the same as the depot - as if the service vehicle is orbiting alongside it. The main specification that must be outlined is the propulsion system. To ensure the use of a HST, a specific impulse of above 15 seconds must be provided. This is made clear through figure 15 as the change in inclination required is 17 degrees or 0.297 radians. As a result of this, a low-thrust thruster was chosen, a Gridded Ion Thruster (NEXT-C) [22].

Table 11: Gridded Ion Thruster (NEXT-C) specifications.

Parameter	**Value**
Thrust range	236 mN
Specific impulse	4190 s

In addition to this, it must be noted that the overall dry mass of the service vehicle will be 1000 kg - including payload.

3.2.2 Far-range Rendezvous

The initial steps that must be taken are inclination and altitude adjustment. The change in inclination is 17 degrees or 0.297 radians. The initial orbit is identical to that of the depot and thus the service vehicle has a velocity of 7.585 km/s at any point along it's orbit. The target satellite is in an elliptical orbit so it's speed varies along its orbital path. At apoapsis (362 km), the target satellite is deemed to have a velocity of 7.689 km/s.

$$\sqrt{3.986 \times 10^5 \left(\frac{2}{6740} - \frac{1}{6736}\right)} = 7.689 km/s$$

To calculate the delta-v required for the HST to the apoapsis point, the following equation can be used [9]:

$$\Delta v = \sqrt{v_1^2 + v_2^2 - 2v_1v_2\cos(\Delta i)} \tag{5}$$

Substituting for given values, a delta-v of 2.26 km/s is found. This is delta-v required to transition the chaser from its initial altitude and inclination to that of at the apoapsis of the target orbit. The substituted equation is shown below and the code is shown in section 7.5.

$$\Delta v = \sqrt{7.586^2 + 7.689^2 - 2 \times 7.5867 \times 7.689 \times \cos\left(\frac{\pi}{180} \times (70 - 53)\right)} = 2.26013 km/s$$

Finally, a single impulse burn at the apogee of the chaser orbit must be completed to place it into the same orbit as the target - essentially completing the first stage of a Hohmann transfer to go from a circular to an elliptical orbit. This is required as for refuelling, a singular intercept point does not provide a sufficient time frame. This manoeuvre will require a delta-v of 0.0034 km/s and is shown below in figure 16.

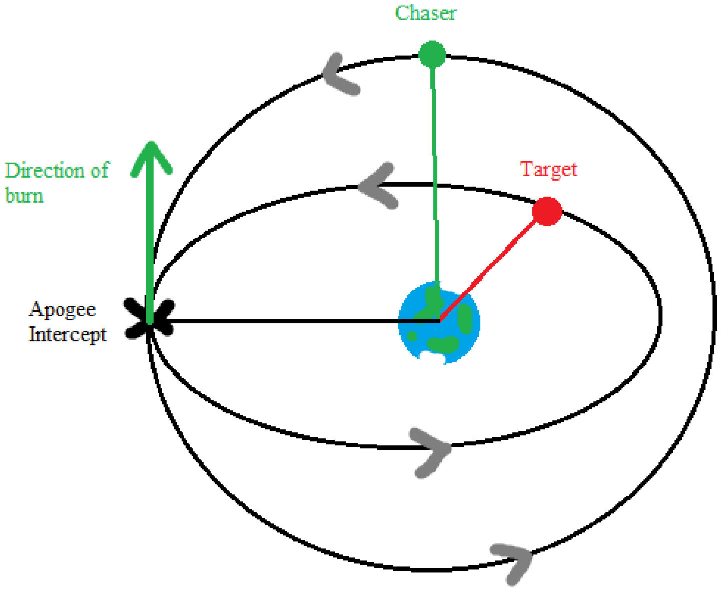

Figure 16: The single impulse transfer between circular and elliptical orbit.

3.2.3 Phasing

For the sake of example, it will be assumed that the chaser satellite is ahead of the target satellite by an angle of 110 degrees - as shown in figure 17

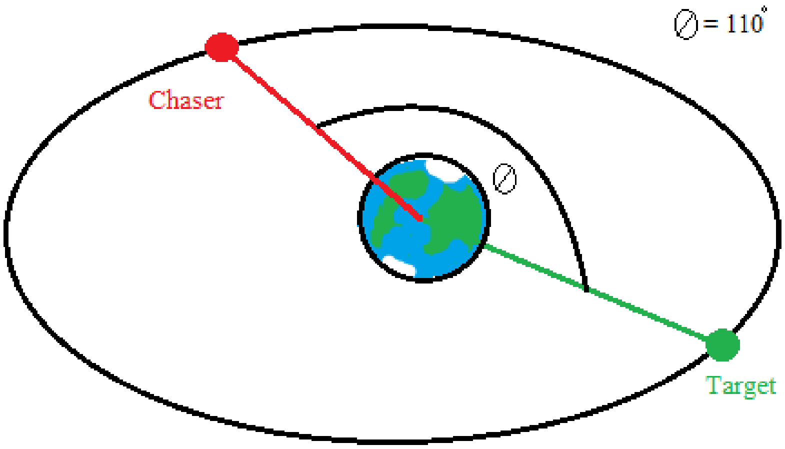

Figure 17: Positions of the chaser and target satellite along an elliptical orbit.

The total delta-v required to complete the phasing is found to be 4.61652 km/s - as per section 7.6.

3.2.4 Total delta-v

The total delta-v associated with the potential rendezvous mission is deemed to be 6.88005 km/s. This is based on the sum of delta-v cost from all phases.

$$\Delta v_{Total} = 2.26013 km/s + 0.0034 km/s + 4.61652 km/s = 6.88005 km/s$$

3.3 Fuel Mass

The fuel cost for the rendezvous can be calculated in the same manner as for the depot satellite - making use of the ideal rocket equation 2.5.

$$m_0 = 1000\,\mathrm{kg} \cdot e^{\frac{6.88005\times10^3\,\mathrm{m/s}}{4190\,\mathrm{s}\times9.81}} = 1182.2057\,\mathrm{kg}$$

Thus, 182.2057 kilograms of fuel is required to perform the rendezvous manoeuvre.

4 Conclusion

Across the depot and service vehicle sections, orbit maintenance and rendezvous manoeuvres have been designed for the '*Beyond Fuel*' on-orbit servicing concept. Making use of simulations, the manoeuvres have been modelled and their fuel costs established.

The depot satellite was determined to maintain an LEO operating altitude of 550km at an inclination of 53 degrees. The depot's lifetime without station keeping was simulated using Python and FreeFlyer - giving an estimation of 50832.5 days. To maintain altitude, station-keeping manoeuvres were designed, this involved the use of Hohmann transfers to raise the depot once it decays 20km away from 550km altitude. Across a 20-year period, 104.2382 kilograms of fuel is required for station-keeping.

An exemplary rendezvous mission with a potential client satellite was designed with the estimated delta-v and fuel costs calculated. The mission consisted of a HST followed by a single impulse and phasing transfer. The mission total delta-v was calculated to be 6.88005 km/s and the fuel cost associated with this was found to be 182.2057 kilograms of fuel. This low fuel cost ensures financial feasibility and is facilitated by the use of low thrust, high specific impulse gridded ion thrusters.

Overall, it is clear that efficient mission design and associated low fuel estimates demonstrate the feasibility of the '*Beyond Fuel*' project. With further innovation, such as updating mission plans to facilitate the servicing of multiple satellites in one mission, the on-orbit servicing model could be scaled up without the need for significant adjustments. This ultimately means a cleaner LEO ecosystem for all and a financially feasible project for the '*Beyond Fuel*' team.

5 Acknowledgements

I am immensely grateful to Dr. Angadh Nanjangud for his invaluable guidance and steadfast support throughout this project. His profound insights and expertise have been instrumental in shaping our work. Dr. Nanjangud's mentorship has greatly contributed to my personal and professional growth, and I am deeply appreciative of the enriching learning experience under his supervision.

6 References

[1] AI Solutions. *Bi-Elliptic Transfer*. Available online at `https://ai-solutions.com/_freeflyeruniversityguide/bi_elliptic_transfer.htm`. Accessed 27 January 2024. 2023.

[2] AI Solutions. *Hohmann Transfer*. Available online at `https://ai-solutions.com/_freeflyeruniversityguide/hohmann_transfer.htm`. Accessed 27 January 2024. 2023.

[3] N. Bannister. "Active Learning in Physics, Astronomy and Engineering with NASA's General Mission Analysis Tool". In: *Journal of Learning and Teaching in Higher Education* 1 (May 2018), pp. 7–30. DOI: `10.29311/jlthe.v1i1.2505`.

[4] *Bipropellant Thrusters Brochure*. `https://www.space-propulsion.com/brochures/bipropellant-thrusters/bipropellant-thrusters.pdf`. Accessed on April 6, 2024.

[5] Yu V Biryukov. "KE Tsiolkovskiy and the first practical steps in Soviet rocketry". In: *Trans. of the first lectures dedicated to the develop. of the SEI. heritage of Ek Tsiolkovskiy Apr. 1970* (1970).

[6] Andrea Capannolo et al. "The space environment". In: *Modern Spacecraft Guidance, Navigation, and Control*. Elsevier, 2023, pp. 77–129.

[7] NASA Glenn Research Center. *Aeronautics - Specifications and Implications*. `https://www.grc.nasa.gov/www/k-12/airplane/specimp.html`. Accessed on April 6, 2024. 2024.

[8] Aerospace Corporation. *Tiangong-1 reentry: Aerospace analysis and recommendations*. Tech. rep. 2018. URL: `https://aerospace.org/sites/default/files/2018-06/Tiangong-1-0318.pdf`.

[9] Howard D Curtis. *Orbital mechanics for engineering students: Revised Reprint*. Butterworth-Heinemann, 2020.

[10] Wigbert Fehse. *Automated rendezvous and docking of spacecraft*. Vol. 16. Cambridge University Press, 2003.

[11] Miguel Fiolhais et al. "Orbital decay in the classroom". In: *The Physics Teacher* 61.3 (2023), pp. 182–185.

[12] Dr Lynnane George. *Introduction to Orbital Mechanics*. PressBooks, 2021. URL: `https://oer.pressbooks.pub/lynnanegeorge/`.

[13] Alan E Hedin. "Extension of the MSIS thermosphere model into the middle and lower atmosphere". In: *Journal of Geophysical Research: Space Physics* 96.A2 (1991), pp. 1159–1172.

[14] Alan E Hedin. "MSIS-86 thermospheric model". In: *Journal of Geophysical Research: Space Physics* 92.A5 (1987), pp. 4649–4662.

[15] RF Hoelker and Robert Silber. "The bi-elliptical transfer between circular co-planar orbits". In: *Army Ballistic Missiles Agency* (1959).

[16] John Kennewell. "Satellite orbital decay calculations". In: *Australian Space Weather Agency* 111 (1999).

[17] Antonio Lira. "How long does it take for a satellite to fall to Earth?" In: *Physics Education* 50.1 (2014), p. 71.

[18] Samuel Low and Yong Xian Chia. “Assessment of orbit maintenance strategies for small satellites”. In: (2018).

[19] J Andrew Marshall and Scott B Luthcke. “Modeling radiation forces acting on TOPEX/Poseidon for precision orbit determination”. In: *Journal of Spacecraft and Rockets* 31.1 (1994), pp. 99–105.

[20] Sara Miller et al. “Survey and performance evaluation of small-satellite propulsion technologies”. In: *Journal of spacecraft and rockets* 58.1 (2021), pp. 222–231.

[21] *MSIS-E-90 Atmosphere Model.* `https://www.ukssdc.ac.uk/wdcc1/msise90.html`. Accessed: March 11, 2024.

[22] NASA Glenn Research Center. *GridDED Ion Thrusters.* `https://www1.grc.nasa.gov/space/sep/gridded-ion-thrusters-next-c/`. Accessed on April 22, 2024.

[23] Victor UJ Nwankwo, Sandip K Chakrabarti, and Robert S Weigel. “Effects of plasma drag on low Earth orbiting satellites due to solar forcing induced perturbations and heating”. In: *Advances in Space Research* 56.1 (2015), pp. 47–56.

[24] J. N. Opiela et al. *Debris Assessment Software Version 2.0.2.* 2012.

[25] *Orbits Catalog.* `https://earthobservatory.nasa.gov/features/OrbitsCatalog`. Accessed: March 7, 2024.

[26] Steven Robert Owens and Malcolm Macdonald. “Hohmann spiral transfer with inclination change performed by low-thrust system”. In: *23rd AAS/AIAA Space Flight Mechanics Conference.* 2013.

[27] Carmen Pardini and Luciano Anselmo. “Monitoring the orbital decay of the Chinese space station Tiangong-1 from the loss of control until the re-entry into the Earth’s atmosphere”. In: *Journal of Space Safety Engineering* 6.4 (2019), pp. 265–275.

[28] T. G. Roberts. *Space Launch to Low Earth Orbit: How Much Does It Cost?* Available online at `https://aerospace.csis.org/data/space-launch-to-low-earth-orbit-how-much-does-it-cost/`. Accessed 27 November 2023. 2022.

[29] *Satellite drag.* `https://www.swpc.noaa.gov/impacts/satellite-drag`. Accessed: November 23, 2023. 2015.

[30] *Section 44: Types of Orbits and Orbital Mechanics.* `https://www.astronomicalreturns.com/p/section-44-types-of-orbits-and-orbital.html`. Accessed: March 7, 2024.

[31] Union of Concerned Scientists. *Satellite Database.* Available at: `https://www.ucsusa.org/resources/satellite-database`. Accessed: February 22, 2024. 2024.

[32] Ranjan Vepa. *Spacecraft Propulsion System Selection.* Lecture Notes. Queen Mary University of London. 2024.

[33] Pauli Virtanen et al. “SciPy 1.0: Fundamental Algorithms for Scientific Computing in Python”. In: *Nature Methods* 17 (2020), pp. 261–272. DOI: `10.1038/s41592-019-0686-2`.

[34] Youcun Wang et al. “Improving Precise Orbit Determination of LEO Satellites Using Enhanced Solar Radiation Pressure Modeling”. In: *Space Weather* 21.1 (2023), e2022SW003292.

7 Appendix

7.1 Project Planner (Gantt chart)

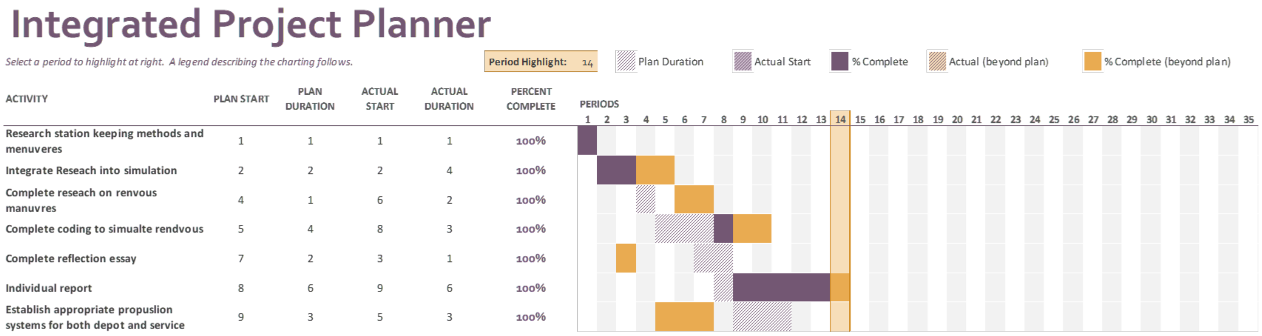

Integrated Project Planner

Select a period to highlight at right. A legend describing the charting follows.

Period Highlight: 14

ACTIVITY	PLAN START	PLAN DURATION	ACTUAL START	ACTUAL DURATION	PERCENT COMPLETE
Research station keeping methods and menuveres	1	1	1	1	100%
Integrate Reseach into simulation	2	2	2	4	100%
Complete reseach on renvous manuvres	4	1	6	2	100%
Complete coding to simualte rendvous	5	4	8	3	100%
Complete reflection essay	7	2	3	1	100%
Individual report	8	6	9	6	100%
Establish appropriate propuslion systems for both depot and service	9	3	5	3	100%

Figure 18: Project Gantt chart with legend.

7.2 Orbital Decay ODE Derivation

Prior to considering orbital decay, an orbit not subject to atmospheric drag must be considered for derivation. In the case of a satellite orbiting around the earth, the force of gravity can be treated as the centripetal force – a fact illustrated by combining the two relevant equations to create equation 8. In this case: F is centripetal force; F_g is the force of gravity; m is the mass of the satellite; M is the mass of Earth; G is the gravitational constant; r is the radius of the orbit from the centre and v is the speed of the satellite.

$$F = \frac{mv^2}{r} \tag{6}$$

$$F_g = \frac{GMm}{r^2} \tag{7}$$

$$\frac{GMm}{r^2} = \frac{mv^2}{r} \tag{8}$$

Equation 8 can be rearranged to solve for the speed of the satellite, as shown below by equation 9.

$$\sqrt{\frac{GM}{r}} = v \tag{9}$$

The conserved mechanical energy of the satellite system, assuming no drag, can be found through equation 8, shown below. This equation combines the gravitational potential energy (equation 6) with the kinetic energy (equation 11).

$$E_{\text{Potential}} = -\frac{GMm}{r} \tag{10}$$

$$E_{\text{Kinetic}} = \frac{1}{2}mv^2 \tag{11}$$

$$E = -\frac{GMm}{2r} \tag{12}$$

The time derivative of the mechanical energy can be written as seen below in equation 13.

$$\frac{dE}{dt} = \frac{d}{dt}\left(-\frac{GMm}{2r}\right) \tag{13}$$

Making use of the chain rule to differentiate, equation 14 can be established – giving a simplified form of the time derivative of mechanical energy.

$$\frac{dE}{dt} = \frac{dr}{dt}\left(-\frac{GMm}{2r^2}\right) \tag{14}$$

When applying this to a system in low earth orbit, atmospheric drag must be accounted for. This drag acts to oppose the velocity of the satellite. The equation for drag force is listed below in equation 15. Within this equation: ρ is local atmospheric density; C_D is the drag coefficient of the satellite; A is the surface area of the satellite and v is the speed of the satellite.

$$F_{\text{Drag}} = \frac{1}{2}\rho C_D A v^2 \tag{15}$$

Subsequent substitution of equation 13 into equation 15 gives the following equation for the magnitude of drag force exerted, as shown below in equation 16.

$$F_{\text{Drag}} = \frac{1}{2}\rho C_D A \left(\frac{GM}{r}\right)^2 \tag{16}$$

The power exerted as a result of the drag force can be calculated through the use of equation 17, resulting in equation 18.

$$P = F_{\text{Drag}} \cdot v \tag{17}$$

$$P_{\text{Drag}} = \frac{1}{2}\rho C_D A \left(\frac{GM}{r}\right)^{3/2} \tag{18}$$

Based on this, the time derivative of mechanical energy can be set equal to the power exerted by drag. This is because the majority of energy change within the system will be associated with drag.

$$\frac{dr}{dt}\left(-\frac{GMm}{2r^2}\right) = P_{\text{Drag}} \tag{19}$$

This equation can be rearranged to give equation 20, making note that $\frac{dr}{dt}$ is represented by $\dot{r}$.

$$\frac{GMm}{2}\frac{\dot{r}}{r^2} = -\frac{1}{2}\rho C_D A \left(\frac{GM}{r}\right)^{3/2} \tag{20}$$

Simplification of this expression allows for the equation to be set for the derivative of altitude from the centre of the earth over time.

$$\dot{r} = -\frac{GMC_D A}{m}\sqrt{r}\rho \tag{21}$$

Equation 21 can be rearranged to provide the altitude of the satellite above the earth instead of from the centre.

$$\dot{h} = -\frac{GMC_D A}{m}\sqrt{R_E + h}\rho \tag{22}$$

This final equation is the ordinary differential equation that when integrated for a specific time, gives the altitude of a chosen satellite above the Earth's surface.

7.3 Orbital Decay Python Script

```python
import numpy as np
import pandas as pd
from scipy.integrate import solve_ivp
import matplotlib.pyplot as plt
import sys

# Constants
G = 6.67430e-11       # gravitational constant (m^3/kg/s^2)
M_EARTH = 5.972e24    # mass of the Earth (kg)
R_EARTH = 6371e3      # radius of the Earth (m)
Cd = 2.2              # drag coefficient
surface_area = 36.55  # satellite surface area (m^2)
mass = 15000          # satellite mass (kg)
minimum = 150000      # rentry altitude (km)

# Load air density data from CSV file
density_data = pd.read_csv(’alt + density 2022.csv’)
heights = density_data[’Altitude’].values *1e3 # convert km to m
densities = (density_data[’Density’].values *1e3)

# Interpolate air density as a function of altitude
density_interp = np.interp

def density_interpolator(h):
        return np.interp(h, heights, densities)

# Effective area and drag constant
A_eff = Cd * surface_area
k = (((G * M_EARTH) ** 0.5) * A_eff) / mass

# ODE for altitude
tolerance = 1  # You can adjust the tolerance based on your needs

def model(t, h):
    if h <= minimum:
        h_dot = 0.0

        if abs(h - minimum) < tolerance:
            days_taken = t/86400   # Assuming ’t’ is the time parameter
            print(f"Altitude dropped below {minimum / 1000} km at t = {days_taken} days.")

        return None

    else:
        density = density_interpolator(h)
        #print(density)
        h_dot = -k * density * (R_EARTH + h) ** 0.5
    return h_dot

# Initial conditions
initial_altitude = float(input("Inital Altitude (km): ")) *10**3   # initial altitude (m)
initial_time = 0.0  # initial time (s)

# Time span for integration
max_time = 60000000000
```

```
steps = 1000
t_span = (initial_time, max_time)
t = np.arange(initial_time, max_time,steps)

# Solve the ODE
solution = solve_ivp(model, t_span, [initial_altitude], method='RK45', t_eval = t,
    dense_output=True)

# Extract results
time_values = solution.t
altitude_values = solution.y[0]

# Plot the results
plt.plot(time_values/86400, altitude_values/1000)
plt.xlabel('Time (Days)')
plt.ylabel('Altitude (km)')
plt.title('Satellite Orbital Decay')
plt.show()
```

7.4 Hohmann Transfer Python Script

```
import math as m
mu = 3.986E5  # km**3/s**2
R_E = 6378  # km

#Inputs
alt_inital= float(input("Altitude tolerance (km): "))  #altitude tolerance (km)
final_alt = float(input("Operational altitude (km): ")) #Operational altitude (km)

#Final orbit
r_final = final_alt + R_E # km
v_final = m.sqrt(mu / r_final)
print('v_final=',v_final,'km/s')

#Initial orbit
r_inital = alt_inital +R_E
v_inital = m.sqrt(mu / r_inital)
print('v_inital=',v_inital,'km/s')

#Transfer orbit
r_per = r_inital
r_apo = r_final
h_t = m.sqrt(2 * mu * r_apo * r_per / (r_apo + r_per))
v_tper = h_t / r_per
v_tapo = h_t / r_apo
print('Perigee and apogee velocity are', v_tper, 'and', v_tapo, 'km/s
    respectively')

#Delta_v
Delta_v = abs(v_final - v_tapo) + abs(v_tper - v_inital)
print('Delta v required is', Delta_v,'km/s')
```

7.5 Hohmann Spiral Transfer Python Script

```
import math

def delta_v(v1, v2, delta_i):
```

```python
    return math.sqrt(v1**2 + v2**2 - 2*v1*v2*math.cos(delta_i))

# Example usage:
v1 = 7.586285640615977  # inital velocity in km/s
v2 = 7.689078116344338  # final velocity in km/s
angle_i = 53 #inital angle in degrees
angle_f = 70 #final angle in degrees
delta_i = math.radians(angle_f-angle_i)  # value for delta_i in radians

result = delta_v(v1, v2, delta_i)
print("Delta-v in km/s is:", result)
```

7.6 Phasing Python Script

```python
import math
#Inputs
Current_period = 91.8 * 60 #seconds
mu = 3.986E5  # km**3/s**2

#Determine how far ahead/behind the target is in time
theta = 110
time_behind = (110/360)*24*3600
print("Time target is behind is:", time_behind,"seconds")

#Determine the period needed for the new orbit
#target is behind the chaser so the chaser needs to slow down.
#This means that we will be expanding our orbit, increasing our SMA, and therefore increasing our period.
New_period = Current_period + time_behind
print("New period is:", New_period,"seconds")

#Calculate the SMA of the new orbit
a_new=(mu*(New_period/(2*math.pi))**2)**(1/3)
print("SMA in km is", a)

#vis-viva - current
mu = 3.986E5
R_E = 6378  # km
apo = 362 + R_E
per = 358 + R_E
r = apo
e = 2.97*10**-4
a = per/(1-e)
v = (mu*((2/r)-(1/a)))**0.5
print(v, "km/s")

#vis-viva - phasing
mu = 3.986E5
R_E = 6378  # km
apo = 362 + R_E
r = apo
v_phasing = (mu*((2/r)-(1/a_new)))**0.5
print(v_phasing, "km/s")

#Calc delta v
#Delta v to rejoin orbit is the same as leaving to multiply by 2
deltav=2*(v_phasing-v)
print(deltav, "km/s")
```